

Entrained flow reactor (EFR)

Gavin Wiggins

June 3, 2020

Contents

1	Introduction	1
2	Experimental setup	2
2.1	Entrained flow reactor	2
2.2	Blend3 feedstock	4
2.3	Forest residue feedstock	6
3	Model development	8
3.1	Pyrolysis kinetics	8
3.2	Biomass characterization	11
3.3	Batch reactor	11
3.4	Sensitivity analysis	11
4	Results and discussion	11
4.1	Blend3 biomass composition	11
4.2	Batch reactor conversion and yields	13
4.3	Sensitivity analysis	13
5	Conclusions	16
6	Source code	16
A	Appendix	16
A.1	Sensitivity analysis	16
	References	18

1 Introduction

This report provides an overview of the Entrained Flow Reactor (EFR) at NREL and associated computational modeling tasks. The reactor operates at fast pyrolysis conditions to thermochemically convert biomass into gaseous products.

The EFR is part of the Thermochemical Process Development Unit (TCPDU) at NREL which was originally designed for biomass gasification where the EFR was used as a thermal cracker. An overview of the TCPDU system is shown in Figure 1.

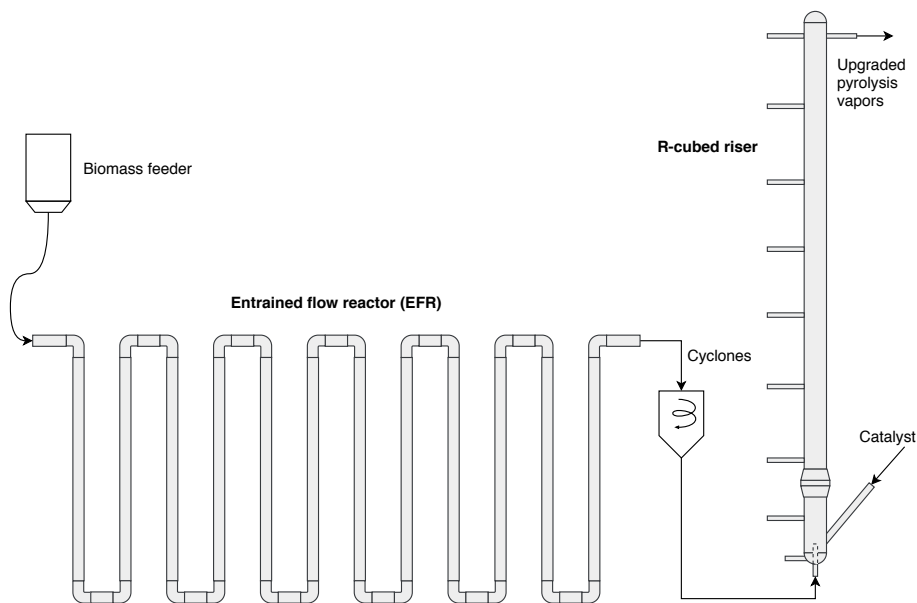


Figure 1: Overview of the main components of the NREL TCPDU system. Fast pyrolysis of biomass occurs in the entrained flow reactor. Catalytic vapor phase upgrading occurs in the R-cubed riser reactor.

2 Experimental setup

This section provides geometric dimensions and typical operating conditions for the entrained flow reactor. Characteristics for the Blend3 and forest residue feedstocks are also discussed.

2.1 Entrained flow reactor

Fast pyrolysis in the TCPDU system occurs in the entrained flow reactor (EFR) which is comprised of a series of horizontal and vertical pipes connected with 90 degree elbows (see Figure 2). The EFR is essentially a pneumatic conveyor where biomass particles flow through a long pipe with several bends. Dimensions and material information about the EFR are provided in Figure 3 below. Operating conditions such as temperatures, pressures, and flow rates for the EFR are shown in Figure 4. Nitrogen gas at 500°C is generally used as the conveying medium for the solids.

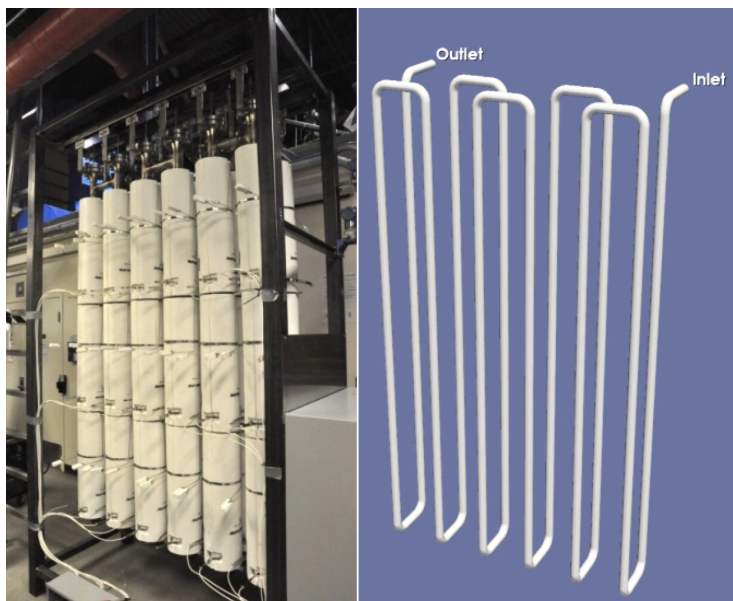


Figure 2: Left - picture of the EFR assembly with heat jackets, insulation, and thermocouples. Right - CAD representation of the EFR pipe assembly used for MFiX simulations.

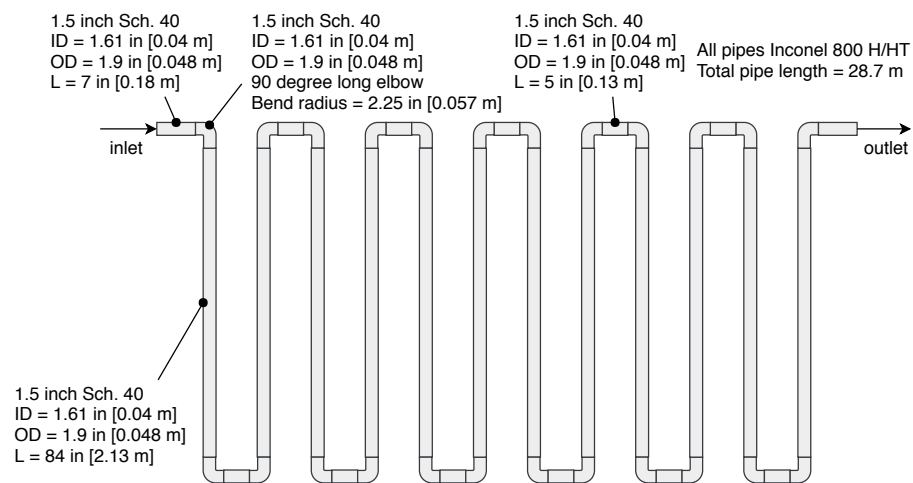


Figure 3: Geometry of the entrained flow reactor at NREL.

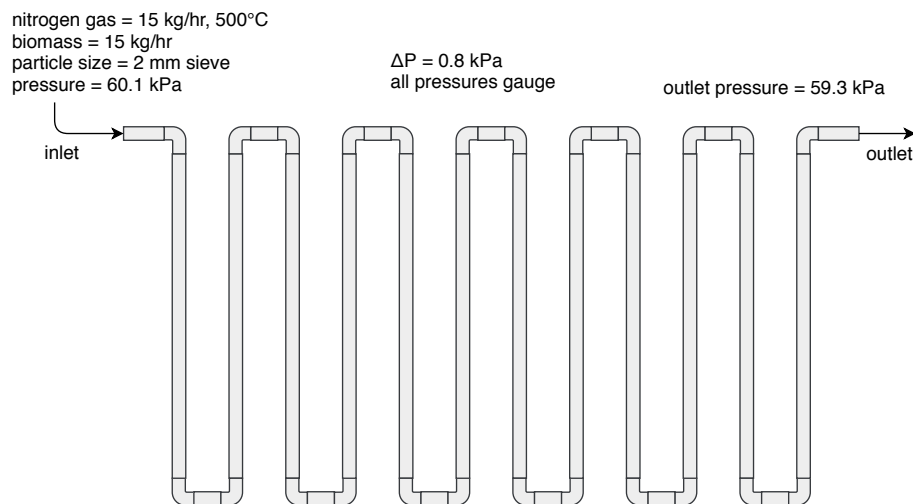


Figure 4: Typical operating conditions for the entrained flow reactor.

2.2 Blend3 feedstock

General information about the Blend3 feedstock used in the entrained flow reactor is provided in Table 1. There is currently no information regarding identification of the feedstock or who performed the feedstock measurements and data preparation. Proximate and ultimate analysis data for the feedstock are presented in Tables 2 and 3. Only one set of analysis data is available therefore the uncertainty in the values is unknown.

Table 1: General information for the Blend3 feedstock.

Item	Description
Name	Blend3
ID	?
Contact	?

Table 2: Blend3 proximate analysis mass percent, as-received basis. Source [3].

Proximate	% ar	% ar	% ar
FC	16.92	?	?
VM	76.40	?	?
ash	0.64	?	?
moisture	6.04	?	?

Table 3: Blend3 ultimate analysis mass percent, as-received basis. Source [3].

Element	% ar	% ar	% ar
C	49.52	?	?
H	5.28	?	?
O	38.35	?	?
N	0.15	?	?
S	0.02	?	?
ash	0.64	?	?
moisture	6.04	?	?

The chemical analysis of the Blend3 feedstock is presented in Table 4. Again, only one set of data is available so the uncertainty in the measurements is unknown. The chemical analysis measurements are used to determine the biomass composition which is needed for the kinetics model.

Table 4: Blend3 chemical analysis mass percent, dry basis. Source [7].

Chemical component	% dry	% dry	% dry
glucan	38.95	?	?
acetyl	1.59	?	?
arabinan	1.40	?	?
galactan	3.16	?	?
mannan	10.52	?	?
xylan	7.89	?	?
lignin	29.48	?	?
free fructose	0.07	?	?
free glucose	0.04	?	?
sucrose	0.04	?	?
water extractives	2.75	?	?
ethanol extractives	3.49	?	?
non-structural inorganics	0.22	?	?
structural inorganics	0.41	?	?

Table 5: Blend3 ash analysis as weight percent of ash. Source [3].

Metal oxide	wt. %	wt. %	wt. %
SiO ₂	28.1	?	?
Al ₂ O ₃	7.06	?	?
TiO ₂	0.34	?	?
CaO	21.8	?	?
Na ₂ O	0.71	?	?
K ₂ O	13.8	?	?
P ₂ O ₅	5.47	?	?
SO ₃	1.23	?	?
Cl	0.09	?	?
CO ₂	5.14	?	?

Table 6: Blend3 particle properties from pelletized crushed feedstock. The crushed feedstock is used in the entrained flow reactor.

Property	Value	Description	Source
ρ	1,050 kg/m ³	particle density, daf basis	[6]
η	0.27	particle porosity	
k	0.23 W/mK	thermal conductivity	

Table 7: Entrained flow reactor yields for Blend3 feedstock.

Yield	wt. %
total liquid	64.9
char	13.9 \pm 0.1
gas	17.2 \pm 0.2
mass balance	96.9 \pm 1.5
carbon balance	93.0 \pm 1.0

2.3 Forest residue feedstock

The forest residue feedstock is comprised of branches/twigs, cambium, needles, bark, and whitewood. This feedstock is used in the NREL fluidized bed reactor (FBR) for the purposes of the FCIC project. The FBR is operated at fast pyrolysis conditions for the thermochemical conversion of biomass. The reactor is sometimes referred to as the 2FBR.

Table 8: General information for the forest residue feedstock.

Item	Description
Name	forest residue
ID	?
Contact	?

Table 9: Bark ultimate analysis mass percent, dry ash-free basis. Source [1].

Element	% daf	% daf	% daf
C	48.27	?	?
H	5.72	?	?
N	0.52	?	?

Table 10: Branches/twigs ultimate analysis mass percent, dry ash-free basis. Source [1].

Element	% daf	% daf	% daf
C	49.69	?	?
H	6.36	?	?
N	0.25	?	?

Table 11: Cambium ultimate analysis mass percent, dry ash-free basis. Source [1].

Element	% daf	% daf	% daf
C	48.52	?	?
H	6.39	?	?
N	0.11	?	?

Table 12: Needles ultimate analysis mass percent, dry ash-free basis. Source [1].

Element	% daf	% daf	% daf
C	48.59	?	?
H	5.92	?	?
N	1.22	?	?

Table 13: Whitewood ultimate analysis mass percent, dry ash-free basis. Source [1].

Element	% daf	% daf	% daf
C	48.27	?	?
H	6.15	?	?
N	0.10	?	?

Table 14: Whitewood biomass composition mass percent, dry basis. Source [2].

Component	% dry
Cellulose	38.04
Hemicellulose	24.2

3 Model development

Details about the biomass pyrolysis kinetics and computational models developed for the entrained flow reactor are discussed in this section.

3.1 Pyrolysis kinetics

The kinetic reaction mechanisms presented by Debiagi et al. are used to model biomass pyrolysis in the entrained flow reactor. These reactions are shown below in Table 15.

Table 15: Kinetic reactions for biomass pyrolysis where A is the prefactor, E is the activation energy, and T is temperature. Source [4].

Item	Reaction	A (1/s)	E (cal/mol)
1	CELL \rightarrow CELLA	1.5×10^{14}	47,000
2	CELLA \rightarrow 0.40 CH ₂ OHCHO + 0.03 CHOCHO + 0.17 CH ₃ CHO + 0.25 C ₆ H ₆ O ₃ + 0.35 C ₂ H ₅ CHO + 0.20 CH ₃ OH + 0.15 CH ₂ O + 0.49 CO + 0.05 G{CO} + 0.43 CO ₂ + 0.13 H ₂ + 0.93 H ₂ O + 0.05 G{COH ₂ } loose + 0.02 HCOOH + 0.05 CH ₂ OHCH ₂ CHO + 0.05 CH ₄ + 0.1 G{H ₂ } + 0.66 CHAR	2.5×10^6	19,100
3	CELLA \rightarrow C ₆ H ₁₀ O ₅	$3.3 \times T$	10,000
4	CELL \rightarrow 4.45 H ₂ O + 5.45 CHAR + 0.12 G{COH ₂ } stiff + 0.18 G{COH ₂ } loose + 0.25 G{CO} + 0.125 G{H ₂ } + 0.125 H ₂	9.0×10^7	31,000
5	GMSW \rightarrow 0.70 HCE1 + 0.30 HCE2	1.0×10^{10}	31,000
6	XYHW \rightarrow 0.35 HCE1 + 0.65 HCE2	1.25×10^{11}	31,400
7	XYGR \rightarrow 0.12 HCE1 + 0.88 HCE2	1.25×10^{11}	30,000
8	HCE1 \rightarrow 0.25 C ₅ H ₈ O ₄ + 0.25 C ₆ H ₁₀ O ₅ + 0.16 FURFURAL + 0.13 C ₆ H ₆ O ₃ + 0.09 CO ₂ + 0.1 CH ₄ + 0.54 H ₂ O + 0.06 CH ₂ OHCH ₂ CHO + 0.1 CHOCHO + 0.02 H ₂ + 0.1 CHAR	$16.0 \times T$	12,900
9	HCE1 \rightarrow 0.4 H ₂ O + 0.39 CO ₂ + 0.05 HCOOH + 0.49 CO + 0.01 G{CO} + 0.51 G{CO ₂ } + 0.05 G{H ₂ } + 0.4 CH ₂ O + 0.43 G{COH ₂ } loose + 0.3 CH ₄ + 0.325 G{CH ₄ } + 0.1 C ₂ H ₄ + 0.075 G{C ₂ H ₄ } + 0.975 CHAR + 0.37 G{COH ₂ } stiff + 0.1 H ₂ + 0.2 G{C ₂ H ₆ }	$3.0 \times 10^{-3} \times T$	3,600

10	HCE2 \rightarrow 0.3 CO + 0.5125 CO ₂ + 0.1895 CH ₄ + 0.5505 H ₂ + 0.056 H ₂ O + 0.049 C ₂ H ₅ OH + 0.035 CH ₂ OHCHO + 0.105 CH ₃ CO ₂ H + 0.0175 HCOOH + 0.145 FURFURAL + 0.05 G{CH ₄ } + 0.105 G{CH ₃ OH} + 0.1 G{C ₂ H ₄ } + 0.45 G{CO ₂ } + 0.18 G{COH ₂ } loose + 0.7125 CHAR + 0.21 G{H ₂ } + 0.78 G{COH ₂ } stiff + 0.2 G{C ₂ H ₆ }	7.0×10^9	30,500
11	LIGH \rightarrow LIGOH + 0.5 C ₂ H ₅ CHO + 0.4 C ₂ H ₄ + 0.2 CH ₂ OHCHO + 0.1 CO + 0.1 C ₂ H ₆	6.7×10^{12}	37,500
12	LIGO \rightarrow LIGOH + CO ₂	3.3×10^8	25,500
13	LIGC \rightarrow 0.35 LIGCC + 0.1 VANILLIN + 0.1 C ₆ H ₅ OCH ₃ + 0.27 C ₂ H ₄ + H ₂ O + 0.17 G{COH ₂ } loose + 0.4 G{COH ₂ } stiff + 0.22 CH ₂ O + 0.21 CO + 0.1 CO ₂ + 0.36 G{CH ₄ } + 5.85 CHAR + 0.2 G{C ₂ H ₆ } + 0.1 G{H ₂ }	1.0×10^{11}	37,200
14	LIGCC \rightarrow 0.25 VANILLIN + 0.15 CRESOL + 0.15 C ₆ H ₅ OCH ₃ + 0.35 CH ₂ OHCHO + 0.7 H ₂ O + 0.45 CH ₄ + 0.3 C ₂ H ₄ + 0.7 H ₂ + 1.15 CO + 0.4 G{CO} + 6.80 CHAR + 0.4 C ₂ H ₆	1.0×10^4	24,800
15	LIGOH \rightarrow 0.9 LIG + H ₂ O + 0.1 CH ₄ + 0.6 CH ₃ OH + 0.3 G{CH ₃ OH} + 0.05 CO ₂ + 0.65 CO + 0.6 G{CO} + 0.05 HCOOH + 0.45 G{COH ₂ } loose + 0.4 G{COH ₂ } stiff + 0.25 G{CH ₄ } + 0.1 G{C ₂ H ₄ } + 0.15 G{C ₂ H ₆ } + 4.25 CHAR + 0.025 C ₂ H ₂ SO ₄ + 0.1 C ₂ H ₃ CHO	1.5×10^8	30,000
16	LIG \rightarrow VANILLIN + 0.1 C ₆ H ₅ OCH ₃ + 0.5 C ₂ H ₄ + 0.6 CO + 0.3 CH ₃ CHO + 0.1 CHAR	$4.0 \times T$	12,000
17	LIG \rightarrow 0.6 H ₂ O + 0.3 CO + 0.1 CO ₂ + 0.2 CH ₄ + 0.4 CH ₂ O + 0.2 G{CO} + 0.4 G{CH ₄ } + 0.5 G{C ₂ H ₄ } + 0.4 G{CH ₃ OH} + 1.25 G{COH ₂ } loose + 0.65 G{COH ₂ } stiff + 6.1 CHAR + 0.1 G{H ₂ }	$8.3 \times 10^{-2} \times T$	8,000
18	LIG \rightarrow 0.6 H ₂ O + 2.6 CO + 0.6 CH ₄ + 0.4 CH ₂ O + 0.75 C ₂ H ₄ + 0.4 CH ₃ OH + 4.5 CHAR + 0.5 C ₂ H ₆	1.5×10^9	31,500
19	TGL \rightarrow C ₂ H ₃ CHO + 2.5 MLINO + 0.5 U ₂ ME ₁₂	7.0×10^{12}	45,700
20	TANN \rightarrow 0.85 C ₆ H ₅ OH + 0.15 G{C ₆ H ₅ OH} + G{CO} + H ₂ O + ITANN	2.0×10^1	10,000
21	ITANN \rightarrow 5 CHAR + 2 CO + H ₂ O + 0.55 G{COH ₂ } loose + 0.45 G{COH ₂ } stiff	1.0×10^3	25,000
22	G{CO ₂ } \rightarrow CO ₂	1.0×10^6	24,500
23	G{CO} \rightarrow CO	5.0×10^{12}	52,500
24	G{CH ₃ OH} \rightarrow CH ₃ OH	2.0×10^{12}	50,000
25	G{COH ₂ }loose \rightarrow 0.2 CO + 0.2 H ₂ + 0.8 H ₂ O + 0.8 CHAR	6.0×10^{10}	50,000
26	G{C ₂ H ₆ } \rightarrow C ₂ H ₆	1.0×10^{11}	52,000
27	G{CH ₄ } \rightarrow CH ₄	1.0×10^{11}	53,000
28	G{C ₂ H ₄ } \rightarrow C ₂ H ₄	1.0×10^{11}	54,000
29	G{C ₆ H ₅ OH} \rightarrow C ₆ H ₅ OH	1.5×10^{12}	55,000
30	G{COH ₂ }stiff \rightarrow 0.8 CO + 0.8 H ₂ + 0.2 H ₂ O + 0.2 CHAR	1.0×10^9	59,000
31	G{H ₂ } \rightarrow H ₂	1.0×10^8	70,000
32	ACQUA \rightarrow H ₂ O	$1.0 \times T$	8,000

Chemical species in the Debiagi et al. kinetic scheme for biomass pyrolysis are listed in Table 16. Species are grouped into solid, metaplastic, gas, and liquid phases.

Table 16: Chemical species in the Debiagi kinetics scheme for biomass pyrolysis. Source [4].

Item	Name	Formula	Phase	Description
1	CELL	C ₆ H ₁₀ O ₅	solid	cellulose
2	CELLA	C ₆ H ₁₀ O ₅	solid	active cellulose
3	GMSW	C ₅ H ₈ O ₄	solid	hemicellulose softwood

4	XYHW	C ₅ H ₈ O ₄	solid	hemicellulose	hardwood
5	XYGR	C ₅ H ₈ O ₄	solid	hemicellulose	grass
6	HCE1	C ₅ H ₈ O ₄	solid	intermediate	hemicellulose
7	HCE2	C ₅ H ₈ O ₄	solid	intermediate	hemicellulose
8	ITANN	C ₈ H ₄ O ₄	solid	intermediate	phenolics
9	LIG	C ₁₁ H ₁₂ O ₄	solid	intermediate	lignin
10	LIGC	C ₁₅ H ₁₄ O ₄	solid	carbon rich	lignin
11	LIGCC	C ₁₅ H ₁₄ O ₄	solid	intermediate	lignin
12	LIGH	C ₂₂ H ₂₈ O ₉	solid	hydrogen rich	lignin
13	LIGO	C ₂₀ H ₂₂ O ₁₀	solid	oxygen rich	lignin
14	LIGOH	C ₁₉ H ₂₂ O ₈	solid	intermediate	lignin
15	TANN	C ₁₅ H ₁₂ O ₇	solid	tannins	
16	TGL	C ₅₇ H ₁₀₀ O ₇	solid	triglycerides	
17	CHAR	C	solid	char as pure	carbon
18	G{COH2} loose	CH ₂ O	metaplastic	loose formaldehyde	
19	G{CO2}	CO ₂	metaplastic	trapped carbon dioxide	
20	G{CO}	CO	metaplastic	trapped carbon monoxide	
21	G{CH3OH}	CH ₄ O	metaplastic	trapped methanol	
22	G{CH4}	CH ₄	metaplastic	trapped methane	
23	G{C2H4}	C ₂ H ₄	metaplastic	trapped ethylene	
24	G{C6H5OH}	C ₆ H ₆ O	metaplastic	trapped phenol	
25	G{COH2} stiff	CH ₂ O	metaplastic	stiff formaldehyde	
26	G{H2}	H ₂	metaplastic	trapped hydrogen	
27	G{C2H6}	C ₂ H ₆	metaplastic	trapped ethane	
28	C2H4	C ₂ H ₄	gas	ethylene	
29	C2H6	C ₂ H ₆	gas	ethane	
30	CH2O	CH ₂ O	gas	formaldehyde	
31	CH4	CH ₄	gas	methane	
32	CO	CO	gas	carbon monoxide	
33	CO2	CO ₂	gas	carbon dioxide	
34	H2	H ₂	gas	hydrogen	
35	C2H3CHO	C ₃ H ₄ O	liquid	acrolein	
36	C2H5CHO	C ₃ H ₆ O	liquid	propionaldehyde	
37	C2H5OH	C ₂ H ₆ O	liquid	ethanol	
38	C5H8O4	C ₅ H ₈ O ₄	liquid	xylofuranose	
39	C6H10O5	C ₆ H ₁₀ O ₅	liquid	levoglucosan	
40	C6H5OCH3	C ₇ H ₈ O	liquid	anisole	
41	C6H5OH	C ₆ H ₆ O	liquid	phenol	
42	C6H6O3	C ₆ H ₆ O ₃	liquid	hydroxymethylfurfural	
43	C24H28O4	C ₂₄ H ₂₈ O ₄	liquid	heavy molecular weight	lignin
44	CH2OHCH2CHO	C ₃ H ₆ O ₂	liquid	propionic acid	
45	CH2OHCHO	C ₂ H ₄ O ₂	liquid	acetic acid	
46	CH3CHO	C ₂ H ₄ O	liquid	acetaldehyde	
47	CH3CO2H	C ₂ H ₄ O ₂	liquid	acetic acid	
48	CH3OH	CH ₄ O	liquid	methanol	
49	CHOCHO	C ₂ H ₂ O ₂	liquid	glyoxal	
50	CRESOL	C ₇ H ₈ O	liquid	cresol	
51	FURFURAL	C ₅ H ₄ O ₂	liquid	2-furaldehyde	
52	H2O	H ₂ O	liquid	water from reactions	
53	HCOOH	CH ₂ O ₂	liquid	formic acid	
54	MLINO	C ₁₉ H ₃₄ O ₂	liquid	methyl linoleate	
55	U2ME12	C ₁₃ H ₂₂ O ₂	liquid	linalyl propionate	
56	VANILLIN	C ₈ H ₈ O ₃	liquid	vanillin	
57	ACQUA	H ₂ O	liquid	water within	biomass

3.2 Biomass characterization

Here.

3.3 Batch reactor

The material balance for a typical chemical reactor is shown in Equation 1 where C_0 is inlet concentration, C is outlet concentration, v is volumetric flow rate, r is the reaction rate, and V is the reactor volume.

$$\begin{aligned} \text{accumulation} &= \text{input} - \text{output} + \text{reaction} \\ \frac{dC}{dt}V &= vC_0 - vC + rV \end{aligned} \quad (1)$$

A batch reactor was modeled to understand the time scales associated with the biomass pyrolysis kinetics. For the batch reactor, input and output is zero therefore only the accumulation and reaction terms remain in the material balance. For a constant volume reactor the V terms cancel out; therefore, Equation 2 represents the material balance for a batch reactor model.

$$\begin{aligned} \text{accumulation} &= 0 - 0 + \text{reaction} \\ \frac{dC}{dt} &= r \end{aligned} \quad (2)$$

3.4 Sensitivity analysis

Here.

4 Results and discussion

Characterization of the biomass along with batch reactor and sensitivity analysis results are discussed in this section.

4.1 Blend3 biomass composition

Several approaches were investigated to characterize the Blend3 feedstock for use with the Debiagi pyrolysis kinetics. The first approach uses the characterization method discussed in the Debiagi et al. 2015 paper where carbon and hydrogen from ultimate analysis is used to determine the biomass composition [5]. To use this approach for the Blend3 feedstock, the mass fraction of C and H on a dry ash-free basis (last column in Table 17) is used for the biomass characterization procedure.

Table 17: Ultimate analysis bases calculated from the Blend3 feedstock as-received data. Mass percent values are given for as-received (ar), dry, and dry ash-free (daf) basis.

Element	% ar	% dry	% daf	% daf
C	49.52	52.70	53.06	53.16
H	5.28	5.62	5.66	5.67
O	38.35	40.82	41.10	41.17
N	0.15	0.16	0.16	
S	0.02	0.02	0.02	
ash	0.64	0.68		
moisture	6.04			

Using a mass fraction of C as 53.16% and H as 5.67%, the Blend3 characterization and reference mixtures are shown in Figure 5 while the estimated biomass composition is given in Table 18. While this approach is useful for limited feedstock data, its accuracy is questionable when compared to experimental measurements. For example, chemical analysis of the Blend3 feedstock measured a lignin composition of 29.48% (see Table 4) whereas the characterization method using ultimate analysis data estimates a total lignin composition greater than 59%.

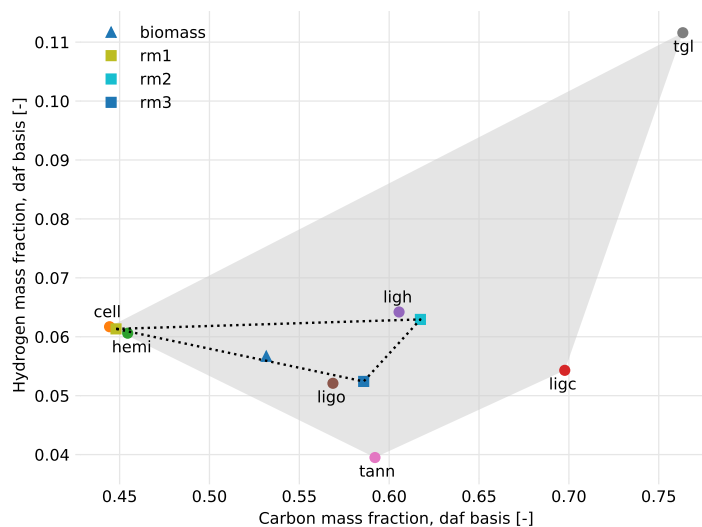


Figure 5: Characterization of the Blend3 feedstock using ultimate analysis data. Reference mixtures (rm) are labeled with square markers.

Table 18: Biomass composition estimated from the Blend3 ultimate analysis data using splitting factors $\alpha = 0.6$, $\beta = 0.8$, $\gamma = 0.8$, $\delta = 1.0$, and $\epsilon = 1.0$.

Biomass composition	% daf
cellulose	26.38
hemicellulose	14.33
lignin-c	7.84
lignin-h	5.27
lignin-o	46.18
tann	0.00
tgl	0.00

Biomass composition for the Blend3 feedstock was estimated from the chemical analysis values given previously in Table 4.

Table 19: Blend3 biomass composition mass percent, dry basis.

Biomass composition	Description	% dry
cellulose	glucan	38.95
hemicellulose	acetyl, arabinan, galactan, mannan, xylan	24.56
lignin	as measured	29.48
tann	here	2.90
tgl	here	3.49
ash	here	0.63

4.2 Batch reactor conversion and yields

Here.

4.3 Sensitivity analysis

Results for the sensitivity analysis of the Debiagi kinetics using a batch reactor model are shown in Tables X.

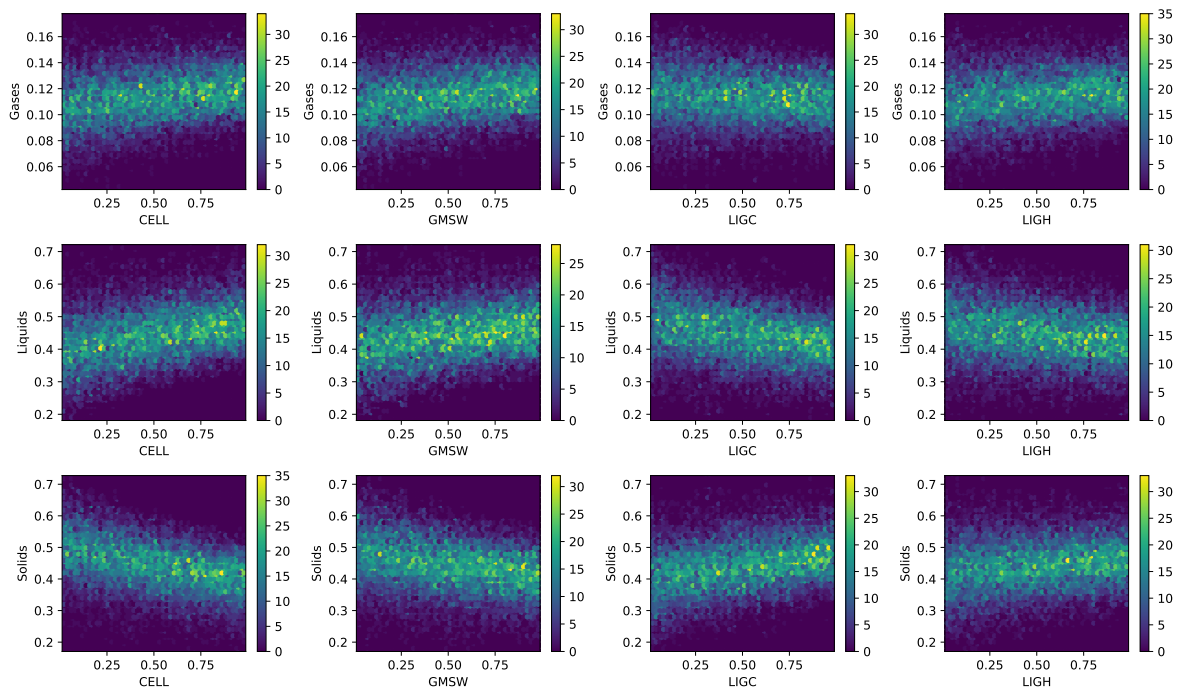


Figure 6: Batch reactor results for cellulose, hemicellulose (GMSW), carbon-rich lignin (LIGC), and hydrogen-rich lignin (LIGH) using 16,000 samples. Reaction time is 10 seconds at 773.15 K and 101,325 Pa. Colorbar represents bin count.

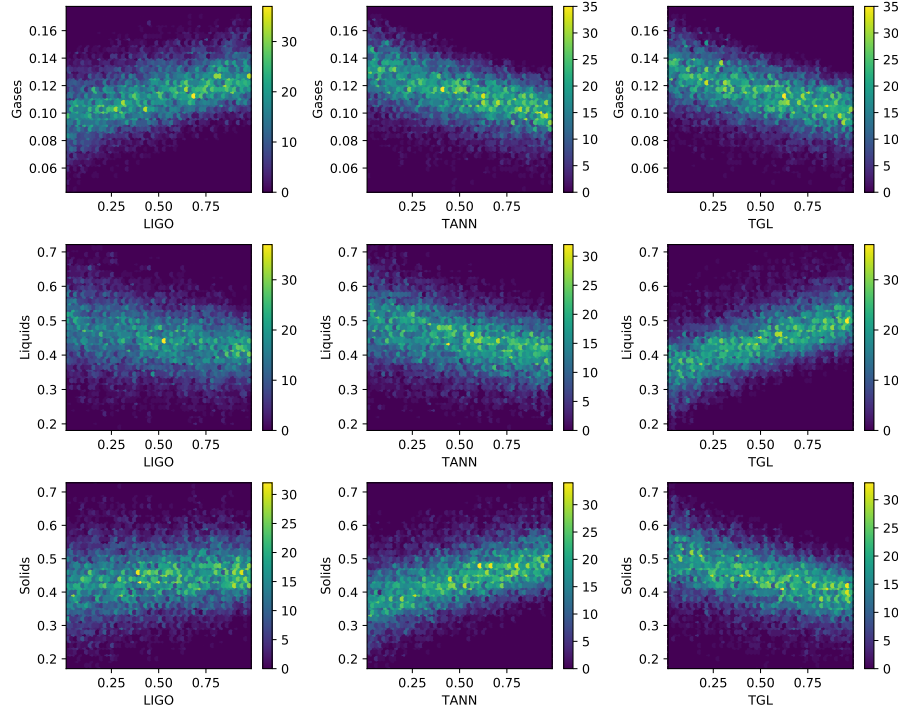


Figure 7: Batch reactor results for oxygen-rich lignin (LIGO), tannins (TANN), and triglycerides (TGL) using 16,000 samples. Reaction time is 10 seconds at 773.15 K and 101,325 Pa. Colorbar represents bin count.

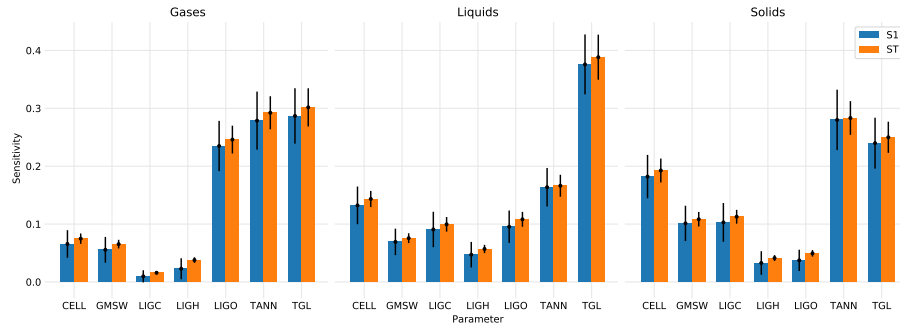


Figure 8: First-order (S1) and total-order (ST) Sobol indices for biomass composition with reactants grouped as gases, liquids, and solids using 16,000 samples.

5 Conclusions

Here.

6 Source code

The Python code used to develop the models and generate results discussed in this paper is available on GitHub at <https://github.com/ccpcode/nrel-efr>.

A Appendix

A.1 Sensitivity analysis

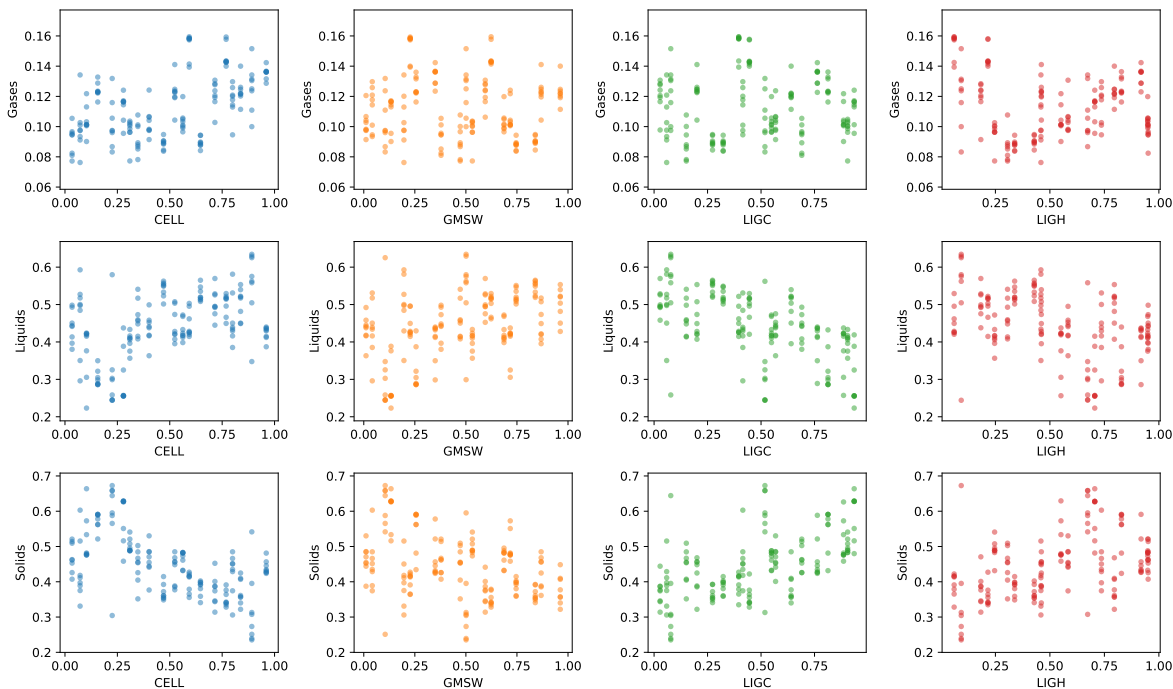


Figure 9: Batch reactor results for cellulose, hemicellulose (GMSW), carbon-rich lignin (LIGC), and hydrogen-rich lignin (LIGH) using 160 samples. Reaction time is 10 seconds at 773.15 K and 101,325 Pa.

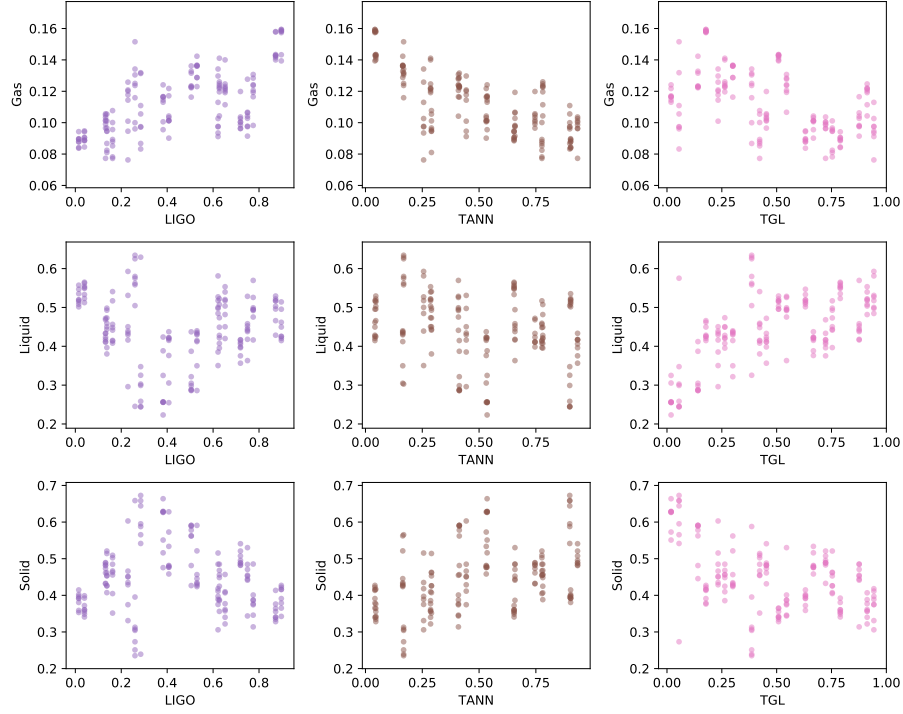


Figure 10: Batch reactor results for oxygen-rich lignin (LIGO), tannins (TANN), and triglycerides (TGL) using 160 samples. Reaction time is 10 seconds at 773.15 K and 101,325 Pa.

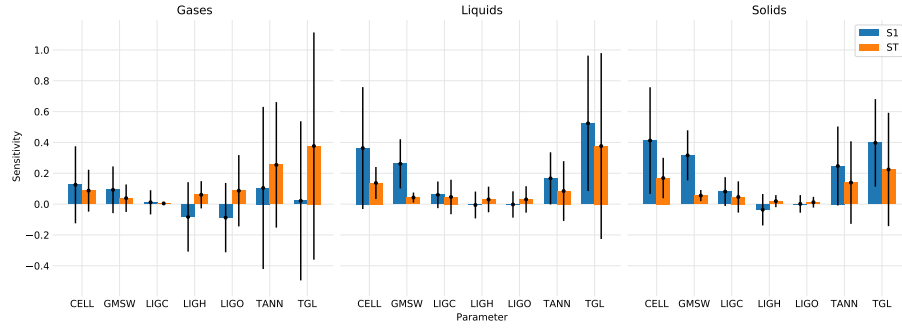


Figure 11: First-order (S1) and total-order (ST) Sobol indices for biomass composition with reactants grouped as gases, liquids, and solids using 160 samples.

References

- [1] Unknown Author. *CHN Analysis Report*. Tech. rep. From Excel spreadsheet `jw-pine-chn-report-jw190920`. Unknown institution, 2019.
- [2] Unknown Author. *Summary normalized*. Tech. rep. From Excel spreadsheet `summary-normalized`. Unknown institution, 2020.
- [3] Mike Choratch. *Proximate and ultimate analysis*. Tech. rep. From PDF `chns_ipc_ms_blend3_nrel2017`. Hazen Research, Inc, 2017.
- [4] P. Debiagi et al. “A predictive model of biochar formation and characterization”. In: *Journal of Analytical and Applied Pyrolysis* 134 (2018), pp. 326–335.
- [5] Paulo Eduardo Amaral Debiagi et al. “Extractives Extend the Applicability of Multistep Kinetic Scheme of Biomass Pyrolysis”. In: *Energy & Fuels* 29.10 (2015), pp. 6544–6555.
- [6] M. Brennan Pecha et al. “Integrated Particle- and Reactor-Scale Simulation of Pine Pyrolysis in a Fluidized Bed”. In: *Energy & Fuels* 32.10 (2018), pp. 10683–10694.
- [7] Anne Starace and Justin Sluiter. *Compositional analysis Blend3*. Tech. rep. From Excel spreadsheet `comp.analysis_blend3_fy17verification`. National Renewable Energy Laboratory, 2020.